

# Study of Heusler compounds $\text{Co}_2\text{YSi}$ ( $\text{Y} = \text{Mn}, \text{Cr}$ ) using a full potential linearized augmented plane wave (FP-LAPW) method

D. P. Rai<sup>1</sup>, Sandeep<sup>1</sup>, A. Shankar<sup>1</sup>, M. P. Ghimire<sup>2</sup>, and R. K. Thapa<sup>1\*</sup>

1. Condensed Matter Theory Group, Department of Physics, Mizoram University,  
Aizawl-796004, India

2. Nepal Academy of Science and Technology, Kathmandu, Nepal

Email: [dibyaprakashrai@gmail.com](mailto:dibyaprakashrai@gmail.com)

Tel: +918014613900, Fax: 0389 - 2330522

**Abstract:** We have performed the volume optimization followed by the calculation of electronic structure and magnetic properties on  $\text{Co}_2\text{MnSi}$  and  $\text{Co}_2\text{CrSi}$ . The structure optimization was based on generalized gradient approximation (GGA) method. The calculation of electronic structure was based on full potential linear augmented plane wave (FP-LAPW) method and exchange correlation. Results of density of states (DOS) and band structures shows the half-metallicity of  $\text{Co}_2\text{MnSi}$  and  $\text{Co}_2\text{CrSi}$  with an integer value of magnetic moments  $5.031 \mu_B$  and  $4.006 \mu_B$  respectively which follows the Slater-Pauling rule.

**Key words:** GGA, LSDA, half-metallicity, DOS and band structure.

**PACS numbers:** 71.15.Mb, 71.15.m, 71.20.-b, 71.15.Ap

## I. Introduction

Half-metallic ferromagnets (HMFs), is a magnetic material where the majority spin band is metallic and the minority-spin band is semiconducting with an energy gap at the Fermi level. In present scientific research of material science, the half-metal ferromagnets have become one of the most studied classes of materials. The existence of a gap in the minority-spin band structure leads to 100% spin polarization of the electron states at the Fermi level which makes the systems applicable for the developing field of spintronics [1]. In half-metals, the creation of a fully spin-polarized current should be possible, that should maximize the efficiency of magnetoelectronics devices [2]. Materials having high spin polarization can be used for tunnel magnetoresistance (TMR) and the giant magnetoresistance (GMR) [3]. The Co-based Heusler alloys  $\text{Co}_2\text{YZ}$  ( $\text{Y}$ : transition metal,  $\text{Z}$ :  $sp$  atom) are the most prospective candidates for the application in spintronics. This is due to a high Curie temperature beyond room temperature and the simple fabrication process such as dc magnetron sputtering in  $\text{Co}_2\text{YZ}$  [4]. Sandeep *et al.* [5, 6] studied the electronic properties of compounds like  $\text{NdCrSb}_3$ ,  $\text{SmCrSb}_3$  and  $\text{GdCrSb}_3$  by first principles method. Ghimire *et al.* [7, 8] studied the electronic properties of  $\text{CrO}_2$  using density functional theory and also studied the electronic

and optical properties of  $\text{SbTaO}_4$ . Rai *et al.* [9, 10] investigated the ground state of  $\text{Co}_2\text{MnAl}$  and  $\text{Co}_2\text{CrSi}$  using LDA+U and LSDA method respectively and reported the half-metallicity. Rai and Thapa have also investigated the electronic structure and magnetic properties of  $\text{X}_2\text{YZ}$  ( $\text{X} = \text{Co}$ ,  $\text{Y} = \text{Mn}$ ,  $\text{Z} = \text{Ge}, \text{Sn}$ ) type Heusler Compounds by using a first Principle Study and reported HMFs [11]. Rai *et al.* (2012) also studied the electronic and magnetic properties of  $\text{Co}_2\text{CrAl}$  and  $\text{Co}_2\text{CrGa}$  using both LSDA and LSDA+U and reported the increase in band gap, hybridization of  $d$ - $d$  orbitals as well as  $d$ - $p$  orbitals when treated with LSDA+U [12]. In this paper we have studied the full-Heusler compounds  $\text{Co}_2\text{MnSi}$  and  $\text{Co}_2\text{CrSi}$  within FP-LAPW method. Our main aim is to investigate the half-metallic behaviour of these compounds, which are a better prospective for the spintronic devices.

## II. Crystal structure and Calculation Details

**2.1 Crystal structure:** Heusler alloy [13] with chemical formula  $\text{Co}_2\text{YSb}$  ( $\text{Y} = \text{Sc}, \text{Ti}$ ), has full Heusler structure with four penetrating fcc sublattices with atoms at  $\text{X1}(1/4, 1/4, 1/4)$ ,  $\text{X2}(3/4, 3/4, 3/4)$ ,  $\text{Y}(1/2, 1/2, 1/2)$  and

$Z(0,0,0)$  positions which results in  $L_{21}$  crystal structure having space group  $Fm-3m$  as shown in Fig-1.

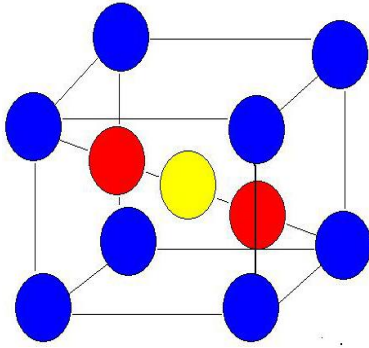


**Fig. 1:** Unit cell Structure of  $Co_2YSi$ : Co (red), Y (yellow) and Si (blue) atoms.

**2.2 Calculation Details:** The FP-LAPW method (WIEN2K) [14] was applied to band structure calculations of  $Co_2CrGe$ . In this method the space is divided into non-overlapping muffin-tin (MT) spheres separated by an interstitial region. The basis functions are expanded into spherical harmonic functions inside the muffin-tin sphere and the Fourier series in the interstitial region. The convergence of basis set was controlled by a cutoff parameter  $R_{MT} \times K_{max} = 7$  where  $R_{MT}$  is the smallest of the MT sphere radii and  $K_{max}$  is the largest reciprocal lattice vector used in the plane wave expansion and made the expansion up to  $l_{max} = 6$  in the muffin tins, where  $l_{max}$  is

the maximum value of angular momentum. The magnitude of the largest vector in charge density Fourier expansion ( $G_{max}$ ) was  $12 \text{ a.u.}^{-1}$ . The cutoff energy which defines the separation of valence and core states was chosen as  $-6.0 \text{ Ry}$ . For k-point sampling, a  $21 \times 21 \times 21$  k-point mesh in the first Brillouin zone was used. LSDA [15] was used and the convergence criterion for self-consistence calculations was set up to charge convergence equal to  $10^{-4}$ . In the interstitial region the charge density and the potential were expands as a Fourier series with wave vectors up to  $G_{max} = 12 \text{ a.u.}^{-1}$ . The MT sphere radii ( $R$ ) used were  $2.35 \text{ a.u.}$  for Co,  $2.35 \text{ a.u.}$  for Cr and  $2.21 \text{ a.u.}$  for Si and in case of  $Co_2MnSi$ ,  $2.34 \text{ a.u.}$  for Co,  $2.34 \text{ a.u.}$  for Mn and  $2.20 \text{ a.u.}$  for Si. The number of k-points used in the irreducible part of the Brillouin zone is 286.

### III. Results and Discussions

The volume optimization was performed using the lattice constant by taking the experimental one. The calculated total energies within GGA as function of the volume were used for determination of theoretical lattice constant and bulk modulus. The bulk modulus was calculated using the Murnaghan's equation of state [16]. The calculated values of lattice constant and bulk modulus are presented in Table 1.

**Table 1:** The previous lattice constant, calculated lattice constant and bulk modulus

Compound	Lattice constant $a_o$ ( $\text{\AA}$ )		Bulk modulus (GPa)
	Previous	Our Calculation	
$Co_2MnSi$	$5.645^{[18]}$	5.665	866.499
$Co_2CrSi$	$5.647^{[17]}$	5.699	405.556

Fig-2 shows the DOS of  $Co_2MnSi$ , at  $-1.4 \text{ eV}$  below  $E_F$  in spin down and spin up regions are contributed by Mn-d atoms but Mn atoms has less contribution in the spin down region. Similarly at  $-1.4 \text{ eV}$ , Co-d atoms also contributed in both spin up and spin down regions. At  $3.2 \text{ eV}$  and  $4.2 \text{ eV}$  in spin down region both Mn-d and Co-d atoms contributed to the total DOS. But negligible contribution from Co and Mn atoms in the spin up channel above  $E_F$ . It is shown in Fig-3 that the hybridization takes place between the Co-d-eg states and Mn-d-eg states below  $E_F$  in the spin up channel, which is responsible for

contribution of magnetic moments. The exchange splitting occurs between the Mn-d electrons at  $-1.8 \text{ eV}$  and  $1.8 \text{ eV}$  is also responsible for the creation of gap in the spin down channel shown in Fig-2(b). From Fig-4(b), in  $Co_2CrSi$  peaks due to Co atoms are found in the valence region for both the spins. In the conduction region sharp peaks were observed at  $0.70 \text{ eV}$  and  $1.8 \text{ eV}$  which were contributed by Co-d states. An exchange splitting also occurs between Co-d up and down with a splitting energy of  $1.4 \text{ eV}$ . In spin down channel, Cr-d contributes both in the valence and conduction regions. We have observed two sharp

peaks -1.4 eV and -2.0 eV in valence region due to Cr-*d* states. An exchange splitting of 2.4 eV is observed between spin down and spin up channel due to Cr-*d* states. This exchange splitting is responsible for the creation of

energy gap as well as magnetic moment. The total magnetic moments and energy gaps of Co<sub>2</sub>MnSi and Co<sub>2</sub>CrSi are given in Table 2.

**Table 2:** The magnetic moments and energy gap are given below.

Compounds	Magnetic Moment $\mu_B$		Energy gap $E_g$ (eV)	
	Previous	Our Calculation	Previous	Our Calculation
Co <sub>2</sub> MnSi	4.900 <sup>[17]</sup> 5.000 <sup>[18]</sup>	5.031	0.798 <sup>[18]</sup>	0.760
Co <sub>2</sub> CrSi	4.000 <sup>[17]</sup>	4.006	0.878 <sup>[17]</sup>	0.910

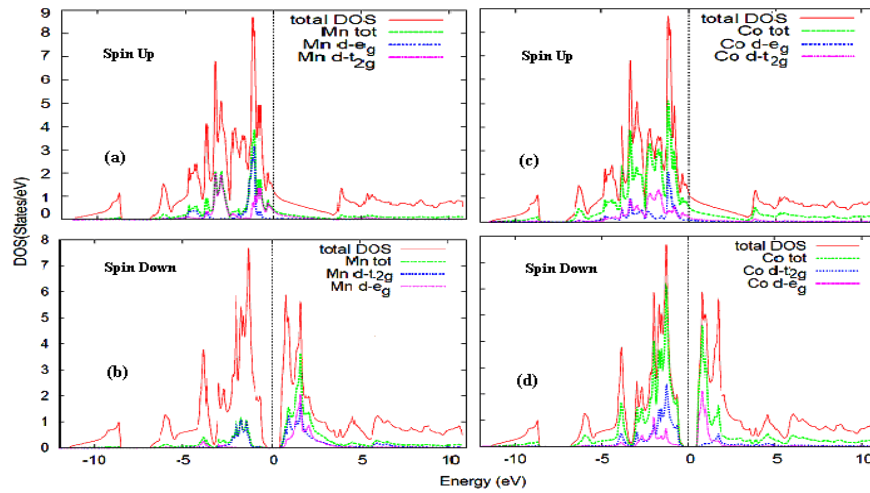


**Fig. 2:** (a) DOS plot for Mn atoms in spin up (b) DOS plot for Mn atoms in spin down (c) DOS plot for Co atoms in spin up and (d) DOS plot for Co atoms in spin down.

The partial magnetic moments of the atoms Co, Mn and Si are 1.029  $\mu_B$ , 3.058  $\mu_B$  and -0.055  $\mu_B$  respectively. Thus the total magnetic moment is 5.031  $\mu_B$  which is approximately an integer value 5.00  $\mu_B$  [18]. There are 9 electrons in the valence shell of Co atoms, 7 electrons for Mn atom, 6 electrons for Cr atom and 4 electrons for Si

atom. According to Slater-Pauling rule [19] the magnetic moment of Co<sub>2</sub>MnSi is  $2 \times 9 + 7 + 4 - 24 = 5 \mu_B$ , similarly 4  $\mu_B$  for Co<sub>2</sub>CrSi which are consistent with our results. The total and partial magnetic moments of Co<sub>2</sub>MnSi and Co<sub>2</sub>CrSi are tabulated in Table 3.

**Table 3:** The partial and total magnetic moments are tabulated and compared with the previous results.

Compounds	Previous Magnetic Moment $\mu_B$			Calculated Magnetic Moment $\mu_B$			
	Co	Y	Total	Co	Y	Si	Total
Co <sub>2</sub> MnSi	1.06	2.99	5.00 <sup>[18]</sup>	1.03	3.06	-0.06	5.031
Co <sub>2</sub> CrSi 0.98	2.08		4.00 <sup>[17]</sup>	0.98	2.10	-0.505	4.006
	1.00	2.03	4.00 <sup>[18]</sup>				

### 3.1. Band Structure

For overall band structure calculation of  $\text{Co}_2\text{MnSi}$  compounds there exist an energy gap  $E_g$  in the spin down region. The width of the energy gap  $E_g$  is the difference of the energies of the highest occupied band in the valence region at the  $\Gamma$ -point and the lowest unoccupied band in the conduction region at the X-point, thus it is an indirect gap. With the help of the DOS, it is clear that the energy region lower than  $-3\text{eV}$  consists mainly of  $s$  and  $p$  electrons of the Si atoms which is called the core and the energy region between  $-3\text{eV}$  and  $2\text{eV}$  consists mainly of the  $d$ -electrons of Co and Mn atoms. Based on the analysis of the band-structure calculation it was shown that the  $3d$

orbitals of Co atoms from two different sub-lattices,  $\text{Co}^1(0, 0, 0)$  and  $\text{Co}^2(1/2, 1/2, 1/2)$ , couple and form bonding hybrids  $\text{Co}^1(t_{2g}/e_g) - \text{Co}^2(t_{2g}/e_g)$ . In other words, the  $t_{2g}/e_g$  orbitals of one of the Co atoms can couple only with the  $t_{2g}/e_g$  orbitals the other Co atom. Furthermore, the Co-Co hybrid bonding orbitals hybridize with the  $\text{Mn}(d)-t_{2g}, e_g$  manifold, while the Co-Co hybrid antibonding orbitals remain uncoupled owing to their symmetry. The Co-Co hybrid antibonding  $t_{2g}$  is situated below the Fermi energy  $E_F$  and the Co-Co hybrid antibonding  $e_g$  is unoccupied and lies just above the Fermi level.

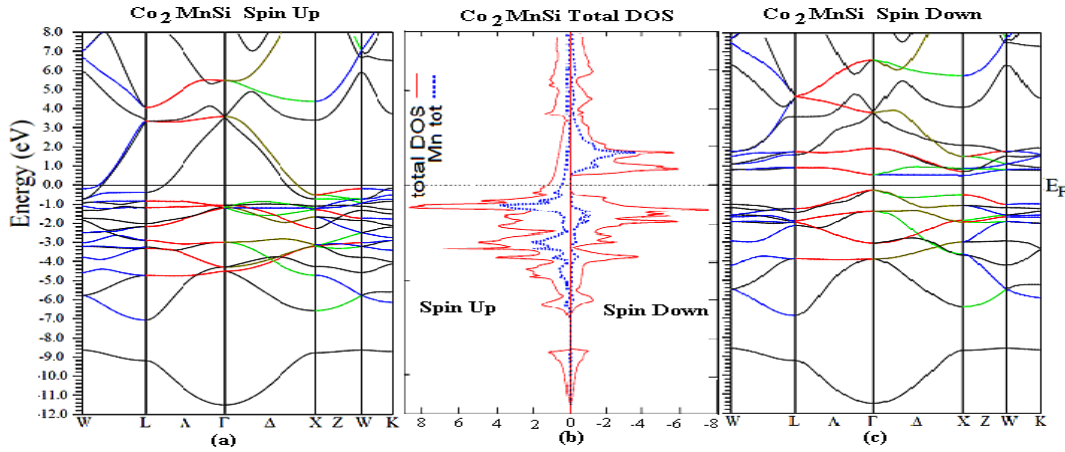


**Fig. 3:** (a) Energy band of  $\text{Co}_2\text{MnSi}$  for spin up (b) Total DOS of  $\text{Co}_2\text{MnSi}$  and (c) Energy band of  $\text{Co}_2\text{MnSi}$  for spin down.

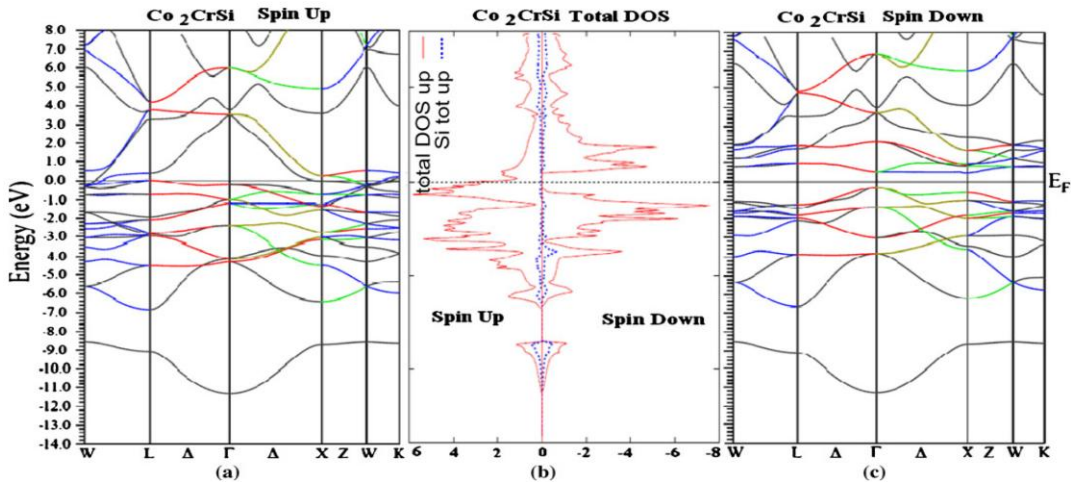


**Fig. 4:** (a) Energy band of  $\text{Co}_2\text{CrSi}$  for spin up (b) Total DOS of  $\text{Co}_2\text{CrSi}$  and (c) Energy band of  $\text{Co}_2\text{CrSi}$  for spin down.

Thus due to the missing Mn(*d*)-*t*<sub>2g</sub>*e*<sub>g</sub> and Co-Co hybrid antibonding hybridization, the Fermi energy is situated within the minority gap formed by the triply degenerate Co-Co antibonding *t*<sub>2g</sub> and the doubly degenerate Co-Co antibonding *e*<sub>g</sub>. From Figs-3 (a-c) it is clearly shown that the E<sub>F</sub> lies exactly at the middle of the gap between the valence and the conduction bands in spin down region where as there is no such gap occur in the spin up region. Thus there exist a half metallicity in Co<sub>2</sub>MnSi. The value of energy gap between  $\Gamma$  and X is 0.760 eV which is an indirect band gap. Almost similar results of 0.798 eV had been reported by Kandpal *et al.* (2006) [18]. From Figs-4(a-c) for Co<sub>2</sub>CrSi, we have observed an indirect band gap in spin down channel. The calculated energy gap along  $\Gamma$ -X symmetry is 0.91 eV which is almost close to 0.878 eV [17].

#### IV. Conclusions

It can be said that due to the existence of gap in DOS for the minority spins, Co<sub>2</sub>MnSi and Co<sub>2</sub>CrSi is a potential half-metallic ferromagnet. This is also evident from the energy band results as discussed. The calculated magnetic moment for Co<sub>2</sub>MnSi is 5.031  $\mu_B$  and 4.006  $\mu_B$  for Co<sub>2</sub>CrSi which is equal to an integer value and follows the Slater-Pauling rule. The integral value of magnetic moment is also one of the evidences for the half metallicity. Due to these characteristics like integer value of magnetic moment, 100% spin polarization at E<sub>F</sub> and the energy gap at the Fermi level in spin down channel makes application of half-metallic ferromagnets very important. The Co-based Heusler alloys Co<sub>2</sub>YZ (Y is transition elements and Z is the sp elements) are the most prospective candidates for the application in spintronics. This is due to a high Curie temperature beyond room temperature and the simple fabrication process such as dc-magnetron sputtering in Co<sub>2</sub>YZ.

#### Acknowledgements

DPR acknowledges DST Inspire fellowship; AS and RKT a research grant from UGC, New Delhi.

#### References

[1] I. Zutic, J. Fabian, S. D. Sarma, Spintronics: Fundamentals and applications, *Rev. Mod. Phys.* 76 (2004), 323–410.  
 [2] de Boeck, W. van Roy, J. Das, V. Motsnyi, Z. Liu, L. Lagae, H. Boeve, K. Dessen, G. Borghs, Technology and

materials issues in semiconductor-based magnetoelectronics, *Semicond. Sci. Technol.* 17 (2002), 342.  
 [3] K. Yakushiji, K. Saito, K. Takanashi, Y. K. Takahashi, K. Hondo, Current-perpendicular-to-plane magnetoresistance in epitaxial Co<sub>2</sub>MnSi/Cr/Co<sub>2</sub>MnSi trilayers, *Appl. Phys. Lett.* 88 (2006), 222504.  
 [4] Y. Miura, K. Nagao, M. Shirai, Atomic disorder effects on half-metallicity of the full-Heusler alloys Co<sub>2</sub>(Cr<sub>1-x</sub>Fe<sub>x</sub>)Al: A first-principles study, *Phys. Rev. B* 69 (2004), 144413.  
 [5] Sandeep, M. P. Ghimire and R. K. Thapa, Electronic and magnetic properties of NdCrSb<sub>3</sub>: A first principles study, *Physica. B* 406 (2011), 1862-1864.  
 [6] Sandeep, M. P. Ghimire and R. K. Thapa, Electronic and magnetic properties of SmCrSb<sub>3</sub> and GdCrSb<sub>3</sub>: A first principles study, *Journal of Magnetism and magnetic materials.* 323 (2011), 2883–2887.  
 [7] M. P. Ghimire, Sandeep and R. K. Thapa, Study of the electronic properties of CrO<sub>2</sub> using density functional theory, *Mod. Phys. Letts. B* 24 (2010), 2187-2193.  
 [8] M. P. Ghimire, Sandeep, T. P. Sinha and R. K. Thapa, First principles study of the Electronic and Optical properties of SbTaO<sub>4</sub>, *Physica B* 406 (2011), 3454–3457.  
 [9] D. P. Rai, J. Hashemifar, M. Jamal, Lalmuanpuia, M. P. Ghimire, Sandeep, D. T. Khathing, P. K. Patra, B. I. Sharma, Rosangliana, R. K. Thapa, Study of Co<sub>2</sub>MnAl Heusler alloy as half metallic Ferromagnet, *Indian J. Phys.* 84 (5) (2010), 593-595.  
 [10] D. P. Rai, Sandeep, M. P. Ghimire, R. K. Thapa, Study of energy bands and magnetic properties of Co<sub>2</sub>CrSi Heusler alloy, *Bull. Mat. Sc.* 34, (2011) 1219-1222.  
 [11] D. P. Rai and R. K. Thapa, Electronic Structure and Magnetic Properties of X<sub>2</sub>YZ (X=Co, Y=Mn, Z=Ge, Sn) type Heusler Compounds: A first Principle Study. *Phase transition: A multinational journal, iFirst*, (2012) 1-11.  
 [12] D. P. Rai, Sandeep, M. P. Ghimire and R. K. Thapa, Electronic structure and magnetic properties of Co<sub>2</sub>YZ (Y = Cr, Y = Al, Ga) type Heusler compounds: A first Principle Study, *Int. J. Mod. Phys. B* 26, 8 (2012) 250071.  
 [13] F. Heusler, Verh. Dtsch. Phys. Ges., Kristallstruktur und Ferromagnetismus der Mangan-Aluminium-Kupferlegierungen, 12 (1903) 219.  
 [14] P. Blaha, K. Schwarz, G. K. H. Madsen, D. Kvasnicka, J. Luitz, K. Schwarz, 2008. An Augmented Plane Wave Plus Local Orbitals Program for Calculating Crystal Properties: Wien2K User's Guide, Techn. Universitat Wien, Wien., 1-108.

- [15] U. Von Barth, L. Hedin, A local exchange-correlation potential for the spin polarized case. I, *J. Phys C:Solid State Phys.* 5 (1972) 1629.
- [16] Murnaghan F D 1944 *Proc. Natl. Acad. Sci. USA*, 30 244
- [17] M. P. Raphael, B. Ravel, Q. Huang, M. A. Willard, S. F. Cheng, B. N. Das, R. M. Stroud, K. M. Bussmann, J. H. Claassen, V. G. Harris, Presence of antisite disorder and its characterization in the predicted half-metal  $\text{Co}_2\text{MnSi}$ , *Phys. Rev. B* 66 (2002) 104429.
- [18] H. C. Kandpal, G. H. Fecher and C. Felser, Calculated electronic and magnetic properties of the half-metallic, transition metal based Heusler compounds, *J. Phys. D: Appl. Phys.* 40, (2006) 1507-1523.
- [19] I. Galanakis, P. H. Dederichs, and N. Papanikolaou, Slater-Pauling behavior and origin of the half-metallicity of the full-Heusler alloys, *Phys. Rev. B* 66, (2002)174429-9.